ACOUSTICS 2012

Visualization and analysis of the vibrations of a human face induced by a bone conduction device using high speed digital holography

M. Leclercq, M. Karray, V. Isnard, F. Gautier and P. Picart

Laboratoire d'acoustique de l'université du Maine, Bât. IAM - UFR Sciences Avenue Olivier Messiaen 72085 Le Mans Cedex 9
mathieu.leclercq.etu@univ-lemans.fr

This paper proposes a first attempt to visualize and analyze the vibrations propagating at the surface of a human face's skin induced by a bone conduction device. The proposed method allows the qualitative visualization and quantitative measurement of the surface movements illuminated by a coherent laser beam. To do this, we developed a new approach in a so-called "quasi-time-averaging regime" allowing the retrieval of the vibration amplitude and phase from a sequence of digital Fresnel holograms recorded with a high image rate. The experimental set-up is based on off-axis digital Fresnel holography and a high power continuous wave laser. The sensor is a high speed CMOS camera permitting recordings with a high spatial resolution (1024×1024 pixels) up to 2.4kHz. The set-up is able to provide full field measurements in the frequency bandwidth 100Hz-600Hz. Recording in the quasi-time-averaging regime leaded to the development of a dedicated algorithm able to extract the vibration using only three holograms from the sequence. The design of the algorithm depends on the ratio between exposure time and vibration period. Results exhibit propagation of vibrations at the skin surface, amplitudes being at most at 200nm, and speed velocity can be estimated at each frequency

1 Introduction

The bone-conduction device, which was created in 2010 by LAUM, is a communication system using the propagation of sound through bones. The station is made up of a vibrator excited by an audio signal, linked to a stalk, whose extremity is in contact with the chin of the user (Figure 1). This set-up constitutes an information terminal and generates an unusual sensorial experience, arousing curiosity and interest from users, either hearing or hearing-impaired people. This station was presented to the public at Pantheon and at Quai Branly Museum, Paris [1].

Figure 1: User with bone conduction device in anechoic room at LAUM

Interaction between the vibrating element and the user's head is not well-known. A better understanding of the transmission mechanism requires the investigation of the vibrations induced by the stalk on the skin of the user's chin. Such a study requires a non-conventional experimental method [2], so as to retrieve a full-field measurement, without any contact and without scanning. This paper proposes a digital holographic interferometer which results in the quantitative analysis of the skin movement with a high speed holographic recording.

2 Different regimes for the recording

An object under a sinusoidal vibration, and illuminated by a coherent beam, produces a spatio-temporal optical phase modulation that can be written as $\Delta\varphi(t)=\Delta\varphi_m\sin(\omega_0 t+\varphi_0)$, where $\Delta\varphi_m$ is the maximum amplitude at pulsation ω_0 (period is $T_0=1/f_0$) and φ_0 is the vibration phase. If the object is illuminated with an incidence angle θ with an optical wavelength λ, the physical amplitude of the vibration can be estimated from the measurement of the optical phase according to (case of out-of-plane vibration):

$$u_z(x,y)=\frac{\lambda}{2\pi}\frac{1}{1+\cos\theta}\Delta\varphi_m(x,y). \quad (1)$$

When studying vibrations of any structure using a digital holographic method [3], it is important to know at which regime recordings are performed. The temporal regime in which holograms are recorded is of primary importance. The characteristic parameter is the cyclic ratio, defined by $\alpha=T/T_0$, which is the ratio between the exposure time T and the vibration period T_0. Its value states the possibility to reconstruct without any error the vibration from a synchronous hologram sequence. In 2005, Leval demonstrated [3] the possibility for the reconstruction of the sinusoidal mechanical vibration from the recording of a sequence including 3 digital holograms. To do this, the holograms must be synchronously phase shifted from the vibration and the cyclic ratio must satisfy $\alpha<1/\Delta\varphi_m$. The value of the cyclic ratio influences the error-free vibration reconstruction from a digital holographic sequence and the different rates are discussed in the next sub-sections.

2.1 Pulsed regime

Typically, if $\alpha<<1$, the recording regime uses light pulses and is equivalent to a freezing of the object at the instant at which the recording is performed ("impulse regime") [4,5,6]. In this case, the condition of short pulse leads to the complex amplitude of the numerically reconstructed object from the recorded digital hologram [3]:

$$\begin{aligned} A_r(x,y) &= TA_0(x,y)\exp\left(i\psi_0(x,y)\right) \\ &\times\exp\left(i\Delta\varphi_m(x,y)\sin\left(\omega_0 t_1+\varphi_0(x,y)+\pi\alpha\right)\right). \end{aligned} \quad (2)$$

$A_0\exp(i\psi_0)$ is the static object amplitude. In such regime, the object is temporally "frozen" and the amplitude

calculated by the holographic process corresponds to the object at the recording time t_1 [6].

2.2 Time-averaging regime

When, on the contrary, we have $\alpha>>1$, the regime is said "time-averaging regime" [7,8,9]. The object reconstructed from the digital hologram is then amplitude-modulated according to:

$$\begin{aligned} A_r(x,y) = A_0(x,y)\exp(i\psi_0(x,y)) \\ \times T\sum_k J_k[\Delta\varphi_m(x,y)]\mathrm{sinc}(k\alpha\pi)\cdot \\ \times\exp[ik(\omega_0 t_1+\varphi_0(x,y)+\pi\alpha)] \end{aligned} \quad (3)$$

where J_k is the Bessel function of first kind of order k. Equation (3) is simplified with the condition of long pulse [7], i.e. $\alpha\to\infty$, according to:

$$A_r(x,y) = TA_0(x,y)\exp(i\psi_0(x,y))J_0(\Delta\varphi_m(x,y)) \quad (4)$$

only depending on $\Delta\varphi_m$ [8]. The nodal lines of the vibration appear to be bright ($\Delta\varphi_m$=0) and the dark fringes are due to the zero-crossing of the J_0 modulation. The computation of the zeros of the J_0 function allows the physical vibration amplitude at each dark fringe to be determined by use of Equation (1) [9].

2.3 Quasi-time-averaging regime

In experiments with $0<<\alpha<1$, the cyclic ratio is too high to be classified as impulse regime and too short to consider the time-averaging regime. This intermediary regime is called here the "quasi-time-averaging regime". Such a regime has not been considered in literature, although vibration analysis using a hologram sequence was described [10]. Equation (3) must be considered without any simplification, with the summation:

$$S = \sum_k J_k[\Delta\varphi_m(x,y)]\mathrm{sinc}(k\alpha\pi)\exp[ik(\omega_0 t_1+\varphi_0(x,y)+\pi\alpha)] \quad (5)$$

Now, the reconstructed object exhibits an amplitude-modulation which depends not only on $\Delta\varphi_m$, but also on φ_0. The position of the bright fringes is not necessarily at $\Delta\varphi_m$=0 and the zeros of the modulation can be shifted. Thus it is necessary to investigate the maxima and the zeros of the modulation according to $\Delta\varphi_m$ and φ_0. As an example, Figure 2 shows $|S|$ versus $\Delta\varphi_m$ and φ_0, for the case α=1/6.

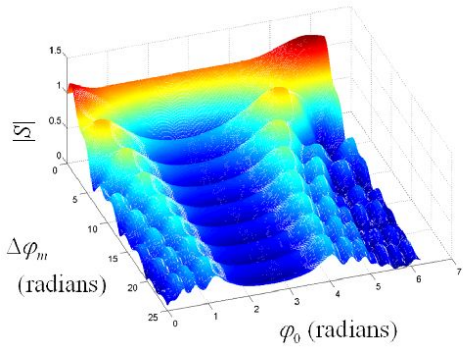

Figure 2: Module of S versus $\Delta\varphi_m$ and φ_0, for α=1/6

Figure 2 shows a succession of maxima and minima, which, as for the time-averaging regime, induces an amplitude modulation on the reconstructed object. The modulation exhibits dark fringes. However, with the quasi-time-averaging regime, minima and maxima vary versus vibration phase φ_0. Thus, two problems appear, that are not encountered with the pure time-averaging regime: first, the first zero of S is not necessarily a first order minimum and it can appear that the succession of maxima and minima is being erroneous due to a second order minimum; last, the first maximum can be not situated at $\Delta\varphi_m$=0. In the time-averaging regime, the first maximum is always localised at the nodal line of the vibration, because the J_0 function is maximum at 0. In the quasi-time-averaging regime, there exists value of φ_0 for which this property is no longer verified. From this, the zero abscissa of the observed fringes will be not at the center of the bright fringe. So the real zero position must be known and value of φ_0 must be known to estimate values of $\Delta\varphi_m$.

These two problems make that the classical approach based on dark fringe counting [9] is obsolete.

However, an approximate dark fringe counting can be applied to roughly estimate the maximum amplitude provided by the vibration. Leval demonstrated that the error-free reconstruction of the vibration is possible from the synchronous recording of a hologram sequence, under the condition that $\alpha<1/\Delta\varphi_m$ ($\Delta\varphi_m$ expressed in radian unit) [3]. Thus, the value of the cyclic ratio is the key for the design of a demodulation algorithm able to provide the vibration amplitude and phase, starting from a sequence recorded in the quasi-time-averaging regime.

3 Demodulation algorithm

With the condition that $\alpha<1/\Delta\varphi_m$, the optical phase extracted from the reconstructed object field, at any instant t_1, is given by $\psi_1=\psi_0+\Delta\varphi_m\sin(\omega_0 t_1+\varphi_0+\alpha\pi)$ (see Equation (2)). Let us consider the recording of a sequence at sampling rate $1/T$. Time for the n^{th} hologram is simply $t_n=t_1+(n-1)T$ and the optical phase is thus $\psi_n=\psi_0+\Delta\varphi_m\sin(\omega_0 t_1+\varphi_0+(2n-1)\alpha\pi)$. From this, the phase difference between two successive reconstructions is $\Delta\psi_n=\psi_{n+1}-\psi_n=2\Delta\varphi_m\sin(\alpha\pi)\cos(\varphi'_0+2n\alpha\pi)$.

Here $\varphi'_0=\omega_0 t_1+\varphi_0$. So, if α can be written in the form $\alpha=1/N$, with N integer, the amplitude and phase of the vibration can be retrieved by this algorithm [11]:

$$\begin{cases} \varphi'_0 = \arctan\left[\dfrac{\sum_{n=1}^{N}\Delta\psi_n\sin(2n\alpha\pi)}{\sum_{n=1}^{N}\Delta\psi_n\cos(2n\alpha\pi)}\right] \\ \Delta\varphi_m = \dfrac{1}{2\sin(\alpha\pi)}\sqrt{\left(\dfrac{2}{N}\sum_{n=1}^{N}\Delta\psi_n\cos(2n\alpha\pi)\right)^2+\left(\dfrac{2}{N}\sum_{n=1}^{N}\Delta\psi_n\sin(2n\alpha\pi)\right)^2} \end{cases} \quad (6)$$

The vibration phase is computed to within about $\omega_0 t_1$. The phase differences $\Delta\psi_n$ are calculated modulo 2π and need to be unwrapped [3]. In the case of recording in the

quasi-time-averaging regime, we have $0<<\alpha<1$, and Equations (6) are suitable only if $\alpha<1/\Delta\varphi_m$.

4 Recording and Reconstruction of digital holograms

In the case of digital Fresnel holography, the object of interest is illuminated by a laser beam with wavelength λ. Thus it diffracts a wave to the recording plane localized at distance d_0, in free space geometry. The object surface generates a wave front that will be noted according to Equation (7):

$$A(X,Y) = A_0(X,Y)\exp[i\psi_0(X,Y)]. \quad (7)$$

Amplitude A_0 describes the object reflectivity and phase ψ_0 describes its surface or shape $\left(i=\sqrt{-1}\right)$. Phase ψ_0 is random and uniformly distributed over the range $]-\pi,+\pi]$. When taking into account the diffraction theory within the Fresnel approximations [12], the object wave diffracted at distance d_0 is expressed by the following relation:

$$\begin{aligned} O(x,y,d_0) = &-\frac{i\exp(2i\pi d_0/\lambda)}{\lambda d_0}\exp\left(\frac{i\pi}{\lambda d_0}\left(x^2+y^2\right)\right) \\ &\times\iint A(X,Y)\exp\left(\frac{i\pi}{\lambda d_0}\left(X^2+Y^2\right)\right) \\ &\times\exp\left(-\frac{2i\pi}{\lambda d_0}(xX+yY)\right)dXdY \end{aligned} \quad (8)$$

Note that since the object is rough, the diffracted field at distance d_0 is a speckle field which has a random and uniform phase over the range $]-\pi,+\pi]$. In the recording plane, the object wave is mixed with a plane reference wave written as:

$$R(X,Y) = a_r\exp(2i\pi(u_0X+v_0Y)). \quad (9)$$

with a_r the modulus and (u_0,v_0) the carrier spatial frequencies. The recording sensor includes $M\times N$ pixels with pitches $p_x=p_y$. We consider here the case of "off-axis digital holography" for which $(u_0,v_0)\neq(0,0)$. The total intensity received by the recording sensor is the digital hologram, written as

$$H = |O|^2 + |R|^2 + OR^* + O^*R. \quad (10)$$

The Shannon theorem applied to off-axis digital holography, resulting in the spatial separation of the three diffraction orders appearing in Equation (10), leads to the optimal recording distance [13]. It is given for a circular object shape with diameter $\Delta A=\Delta A_x=\Delta A_y$:

$$d_0 = \frac{\left(2+3\sqrt{2}\right)p_x}{2\lambda}\Delta A. \quad (11)$$

Ideally, the spatial frequencies of the reference wave must be adjusted to $(u_0,v_0)=(\pm(1/2-1/(2+3\sqrt{2}))/p_x,\pm(1/2-1/(2+3\sqrt{2}))/p_y)$ for the circular object [13].

The reconstructions of the amplitude and the phase of the encoded object are based on the numerical simulation of light diffraction. For a reconstruction distance equal to $d_r=-d_0$, the reconstructed field A_r is given by the discrete version of Equation (8) (known as S-FFT algorithm, or also DFT: discrete Fresnel transform) [1,13,14]. If the reconstructed plane is computed with $(K,L)\geq(M,N)$ data points, then the sampling pitches in the reconstructed plane are equal to $\Delta\eta=\lambda d_0/Lp_x$ and $\Delta\xi=\lambda d_0/Kp_y$ [1,14]. The reconstructed field is given by the following relation, the unnecessary factors and phase terms being removed.

$$\begin{aligned} &A_r(n\Delta\eta,m\Delta\xi) = \\ &\sum_{k=0}^{k=K-1}\sum_{l=0}^{l=L-1}H(lp_x,kp_y)\exp\left[-\frac{i\pi}{\lambda d_0}\left(l^2p_x^2+k^2p_y^2\right)\right]\exp\left[2i\pi\left(\frac{\ln}{L}+\frac{km}{K}\right)\right] \end{aligned} \quad (12)$$

where l, k, n, m are indices corresponding to discrete versions of respectively X, Y, x, y. Due to Shannon conditions, the minimum distance that can be put in the algorithm is given by $d_0\geq\max\{Np_x^2/\lambda,Mp_y^2/\lambda\}$. The computation leads to complex-valued results, from which the amplitude image (modulus) and the phase image (argument) can be extracted.

5 Experimental set-up

The experimental set-up is described in Figure 3. The laser is a continuous wave green laser (λ=532nm) with maximum power at 2W. The human face (illuminated with angle θ=3°) is placed at d_0=1900mm from the sensor. The inspected zone is about $\Delta A_x\times\Delta A_y=80\times80mm^2$. A high speed CMOS sensor (1024×1024 pixels, pitches $p_x=p_y$=14.8µm), can record hologram sequences at $1200s^{-1}$. The digital holograms are reconstructed with the discrete Fresnel transform with 2048×2048 pixels.

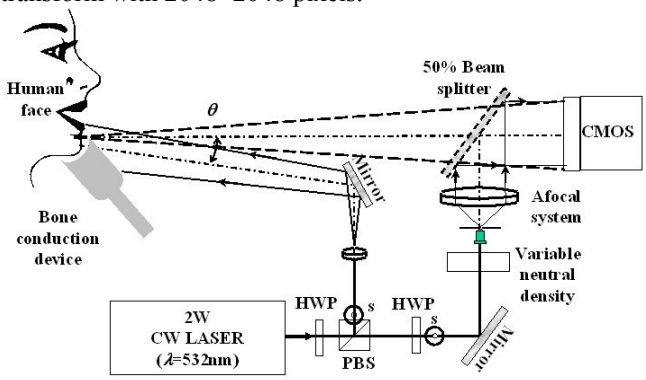

Figure 3: Experimental setup

Figure 4 exhibits a photograph of the human face positioned on the bone-conducting device and illuminated by the cw laser.

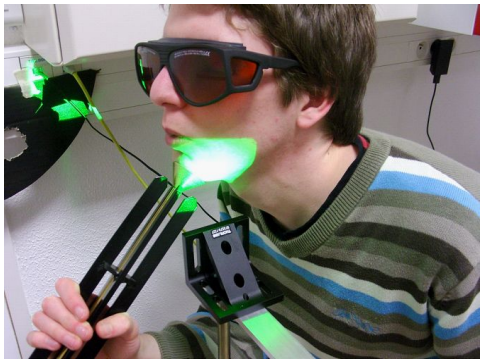

Figure 4: Human face illuminated by the laser

6 Experimental results

The excitation signal provided to the device is harmonic. Sequences with 1s duration are recorded for different sound frequencies at maximum excitation amplitude authorized by the device. Recording is performed in the quasi-time-averaging regime with cyclic ratio in the form of $\alpha=1/N$. Figure 5 shows the reconstructed zone with cyclic ratio $\alpha=1/4$, $f_0=300$Hz at $1200s^{-1}$, in which one can see the excitation cone (defined by points A, B,C), the skin of the chin and the Bessel fringes due to the quasi-time-averaging regime. Figure 6 exhibits a sequence of 30 images extracted from the full sequence, and exhibits the evolution of dark and bright fringes.

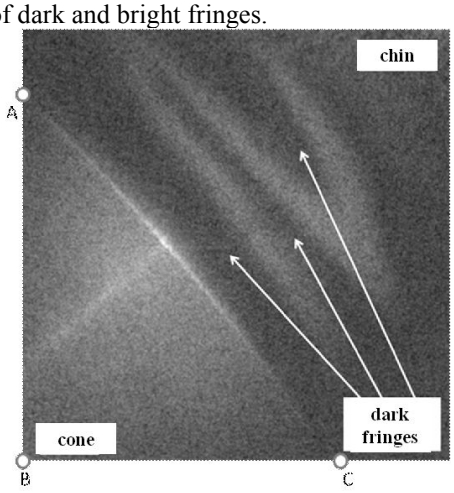

Figure 5: Reconstructed zone with α=1/4

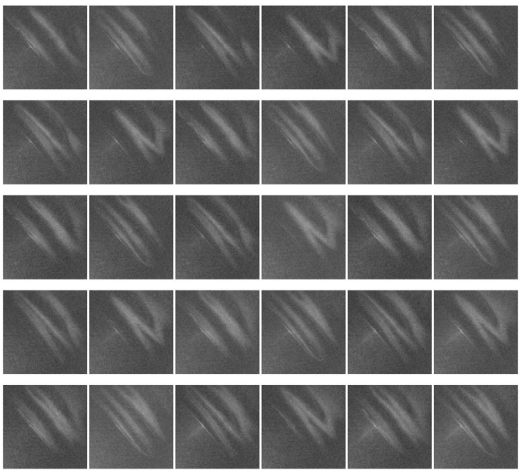

Figure 6: Sequence representative of 30 images with α=1/4

The validity condition for Equation (6) is $\Delta\varphi_m<4$rad. The analysis of the structure of the Bessel fringes in Figure 6 shows that the maximum evaluated amplitude is not greater than 4rad. So algorithm of Equation (6) can be applied to extract amplitude and phase of the vibration at the skin surface. Figure 7 shows the amplitude map of the vibration at the surface of the human skin, computed from Equation (6), when taking into account the illumination conditions. Amplitude is included in the range 60-160nm. At this frequency, the measurement of the spatial periodicity leads to estimate the sound velocity at about $1.42m.s^{-1}$.

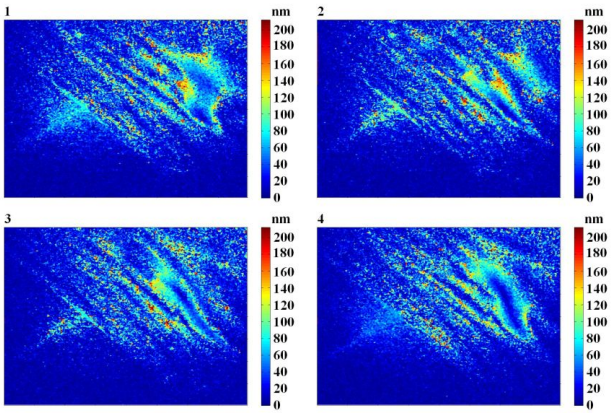

Figure 7: Physical amplitude of the vibration over a period of 3.3ms for $\alpha=1/4$

Figure 8 shows the reconstructed zone with cyclic ratio $\alpha=1/6$, $f_0=200$Hz at $1200s^{-1}$. The validity condition for Equation (6) is $\Delta\varphi_m<6$rad. The analysis of the structure of the Bessel fringes in Figure 8 shows that the maximum evaluated amplitude is not greater than 6rad.

Figure 8: Reconstructed zone with α=1/6

Figure 9 shows the amplitude map of the vibration at the surface of the human skin, computed from Equation (6).

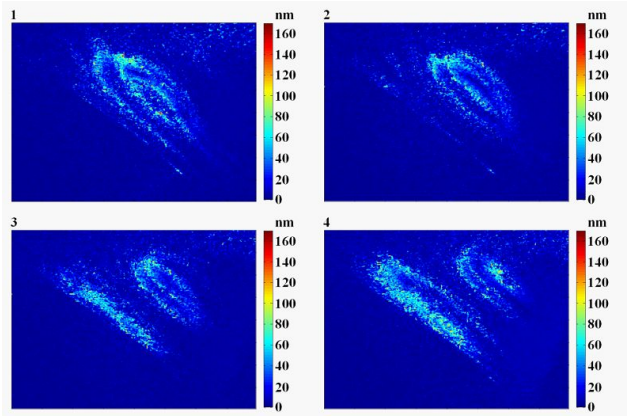

Figure 9: Physical amplitude of the vibration over a period for α=1/6

Amplitude is included in the range 20-100nm The measurement of the spatial periodicity leads to estimate the sound velocity at about 1.62m.s^{-1}.

In order to estimate the sound velocity in the skin media, the distance between two consecutive bright fringes is measured for several consecutive measurements, retrieving this way the averaged spatial wavelength of the oscillations λ_{osc} for each frequency f_0 of the excitation. The sound velocity is then obtained by multiplying the measured spatial wavelength by the excitation frequency according to $v_{osc}=\lambda_{osc}f_0$. Figure 10 shows the calculated velocity for each frequency, with the errors bars retrieved from averaging each measurement.

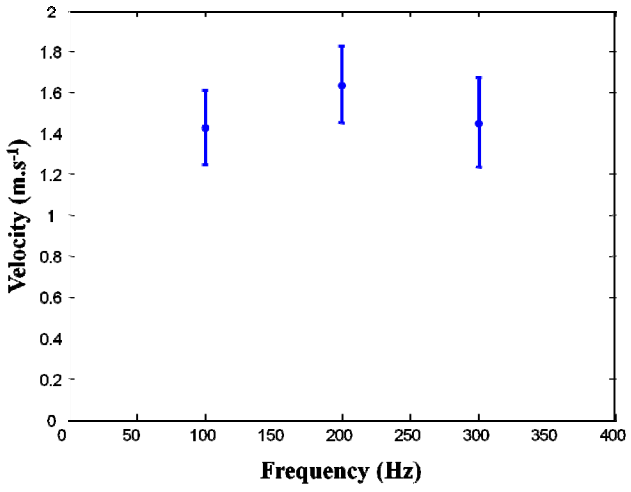

Figure 10: Measured sound velocity vs frequency

7 Conclusion

The paper proposes the use of the quasi-time-averaging regime to visualize and analyze the vibrations induced by a bone-conduction device and propagating at the surface of a human skin. Such a recording leads to the development of a dedicated algorithm, depending on the ratio between exposure time and vibration period. Experimental results permit to estimate the velocity of the sound propagating at the surface of the human face, and due to the excitation provided by the bone conduction device. These results constitute a first attempt in applying digital holography to the field of bio-acoustics.

References

[1] http://www.cnrs.fr/insis/recherche/docs-evenements/ecouter-autrement.pdf

[2] U. Schnars, W. Juptner, "Direct recording of holograms by a CCD target and numerical reconstruction", Applied Optics 33, 179-181 (1994)

[3] J. Leval, P. Picart, J.-P. Boileau, J.-C. Pascal, "Full field vibrometry with digital Fresnel holography", Applied Optics 44, 5763-5771 (2005)

[4] G. Pedrini, H. Tiziani, Y. Zou, "Digital double pulse-TV holography", Optics & Lasers in Engineering 26, 199-219 (1997)

[5] G. Pedrini, Ph. Froening, H. Fessler, H. Tiziani, "Transient vibration measurements using multipulse digital holography", Optics & Laser Technology 29, 505-511 (1997)

[6] P. Picart, J. Leval, F. Piquet, J.-P. Boileau, Th. Guimezanes, J.-P. Dalmont, "Tracking high amplitude auto-oscillations with digital Fresnel holograms", Optics Express 15, 8263-8274 (2007)

[7] R.L. Powell, K.A. Stetson, "Interferometric analysis by wavefront reconstruction", JOSA A 55, 1593-1598 (1965)

[8] P. Picart, J. Leval, D. Mounier, S. Gougeon, "Time averaged digital holography", Optics Letters 28, 1900-1902 (2003)

[9] P. Picart, J. Leval, D. Mounier, S. Gougeon, "Some opportunities for vibration analysis with time-averaging in digital Fresnel holography", Applied Optics 44, 337-343 (2005)

[10] Y. Fu, G. Pedrini, W. Osten, "Vibration measurement by temporal Fourier analyses of a digital hologram sequence", Applied Optics 46, 5719-5727 (2007)

[11] J.E. Greivenkamp, "Generalized data reduction for heterodyne interferometry", Optical Engineering 23, 350-352 (1984)

[12] J.W. Goodman, *Introduction to Fourier Optics*, Second Edition, McGraw-Hill Ed., New York (1996)

[13] P. Picart, J. Leval, "General theoretical formulation of image formation in digital Fresnel holography", JOSA A 25, 1744-1761 (2008)

[14] Th. Kreis, M. Adams, W. Jüptner, "Methods of digital holography: a comparison". Proceedings SPIE 3098, 224-233 (1997)